This article has been accepted for publication in a future issue of this journal, but has not been fully edited.
Content may change prior to final publication in an issue of the journal. To cite the paper please use the doi provided on the Digital Library page.

Self Powered Autonomous Underwater Vehicles (AUVs): Results from a gyroscopic energy scavenging prototype

N.C. Townsend

Abstract

This paper describes and presents preliminary experimental results from a novel prototype energy scavenging system installed in a model 2m cylindrical Autonomous Underwater Vehicle (AUV).

The system, which is based on control moment gyroscope (CMG) principles, utilises the gyroscopic response of a gimballed flywheel mounted within an AUV body to generate energy from the wave induced rotational motions of the vehicle. This method, of using the reaction of a spinning wheel under an input torque to provide an output torque of greater magnitude, orthogonal to the input torque axis and the spin axis provides a means to harvest energy in-situ, without external appendages and additional hydrodynamic drag. The system promises to extend AUV mission durations indefinitely and reduce support vessel time currently required for periodical recharging and redeployment.

A description of the system operation, design and experimental results from a series of regular wave tests conducted at zero speed in a towing tank are presented in this paper. The results show that the system can harvest energy, with greatest power generation around resonance, tailing off as the frequency increases and typically nonlinear in nature. The results show that the system could provide additional hotel load or power specific systems on an AUV and potentially any rotationally excited platform, e.g., Autonomous Surface Vessels (ASVs), Buoys or Boats.

Index Terms

AUVs, ASVs, Energy scavenging, Energy harvesting, Renewables, Power, Gyroscopic, Gyroscopes

I. Introduction

Autonomous Underwater Vehicles (AUVs) have limited endurance capabilities [51]. Nearly all AUVs depend on stored energy for their operation [41]. Currently, the majority of AUVs use batteries as an energy supply for their operation [42], [51]. However, batteries have a finite life (stored energy), require periodical recharging (and redeployment) from a dedicated host platform or support vessel and represent a significant proportion of the total vehicle mass, typically around 20% [41]. A summary of various AUV sensors and AUV power requirements is given in Table I and II. With current AUV endurance, measured in hours or days [36], alternative power systems or in-situ charging strategies are required to extend missions.

With most of the oceans containing an average wind power density greater than 50 W/m^2 for more than 80% of the year (with a maximum of 1600 W/m^2) [55], an average solar energy power density at the surface of approximately 168 W/m^2 (approximately 1270 W/m^2 at the limits of the atmosphere) [44] and the global oceans containing a wave energy density greater than 2 kW/m for 90% of the year (and wave energy densities greater than 20 kW/m in mid-latitudes) [58], the available ambient power is comparable to that required by an AUV. That is, energy scavenging systems, in particularly wave energy scavengers, promise to; enable AUV systems to be remotely and renewably recharged at sea, extend mission durations and capabilities, negate the necessity to carry sufficient energy reserves (size and weight) for entire mission(s), reduce costs by freeing support vessel time (a major cost component in AUV deployment) and provide flexibility in system deployment and recovery (time and/or location).

Solar powered AUVs and several solar assisted commercial ASVs systems e.g., SAUV-II [38], Autonaut [5], WaveGlider [17] and C-Enduro [4], have been developed. While solar potentially offers unlimited mission durations, as found by the SAUV II it is limited to night-time missions and daylight recharging strategies and is susceptible to bio fouling [38]. A prototype thermal energy harvesting underwater vehicle, the SOLO-TREC, has also been developed, which uses a phase-change material (a waxy fluid) that melts and expands in warm water (at the surface) and solidifies in cooler (deeper) water to drive a hydraulic generator and provide power [57]. The SOLO-TREC is reported to provide over 7000 Joules per dive, sufficient to power GPS, Iridium and Conductivity-Temperature-Depth (CTD) Sensors [57]. In the past internal combustion engines have been used to power AUVs. However, these systems were found to be limited as additional power is needed to expel the exhaust gases at depths greater than 200m [51]. Fuel cells have also been trialled, for example on the AUV URASHIMA [45] and IDEF Ifremer [50], however, these systems are expensive and complex [50]. The Royal Swedish Navy has used Stirling engines

TABLE I
EXAMPLE AUV SENSOR POWER REQUIREMENTS

Sensor	Power [W]
Pressure Sensor	0.1 (typ) [22]
Digital compass	0.132 (typ) 0.014 (sleep) [9]
Sound Velocity sensor	0.25 (typ) [29]
Echo Sounder	0.25 (max) [12]
Fluorometer	0.3 (typ) [8]
Precision timing reference	0.3 (max) [14]
Hydrophone	0.12 to 0.3 (typ) [26]
MEMS AHRS and GPS/INS	0.675 to 0.95 (typ) [31]
Turbulence Sensor	1 (typ) [19]
2D imaging sonar	3 (typ) [2]
Conductivity Temperature Depth (CTD) Sensor	3.42 (incl. pump) [23]
Digital Camera	5 (typ) [11]
Sidescan sonar	5 (typ exclude CPU) [24]
LBL Acoustic Positioning System	2.5 to 5.5 (transmit), 1.3 (max receive) 0.005 to 0.285 (listen mode) 0.0025 (standby) [16]
Nitrate Sensor	7.5 (max) [27]
Doppler velocity log	12 (max transmit) 2(average transmit) 1.1(typ) [10]
3D imaging sonar	15 (typ) [18]
Underwater RF	16 (transmit) 5 (receive) 0.005 (sleep) [30]
Current Profiler	20 to 0.3 (Transmit) 0.2 to 1.4 (typ) [3]
Side scan sonar and Sub bottom profiler	30 (max) [1]
Navigation and control system	50 (max) 2 (active listening) 0.7 (sleep) [7]
Multibeam Swath Bathymetry and Sidescan	50 (max) 20 (standby) [13]
Transponder	50 (max) 2 (active) 0.7 (sleep) [6]
Underwater laser scanner	144 (typ) [28]
Acoustic Communications	300 (transmit) 1.8 (receive/standby) 0.08 (standby) [15]

[51] and (Slocum) gliders have been developed using ocean temperature gradients and battery power to provide propulsion [39]. Various wind based concepts, for example C-enduro and the Submaran [21], are being developed. The C-enduro uses a deck mounted wind turbine to generate power and the Submaran uses a fixed wing (sail) for propulsion. Various sail based systems have also be developed for the Microtransat Challenge [20] - a fully autonomous sailing boat transatlantic race. Interestingly, no successful transit of the Atlantic within this competition has been made to date. Ideas of recharging AUV power supplies using wave-energy absorbers and sea current generators have also been proposed [37], [43], however, no practical demonstrations have been made. While wave propelled devices, for example the Autonaut and Wave Glider have been developed, these systems do not currently generate power. To date no wave energy scavenging systems have been demonstrated.

This paper reports the results from the first demonstration of a gyroscopic wave based energy scavenging system for an AUV. Currently gyroscopic wave energy converters (WECs) are gaining interest with several systems being developed in Japan [46]–[48], Italy [33]–[35] and Spain [52]. Unlike the systems being developed in Italy and Spain, with large, slow flywheels with limited precession and horizontal precession axis and the large (kW scale) WEC systems being developed in Japan, this study demonstrates;

- A small scale system specifically for energy scavenging applications,
- A system with a vertical precession axis (whereby the rolling and pitching motions contribute to the energy harvested)
- A system with high flywheel rpm (thousands not hundreds)
- A system with unrestricted precession motion (where the gyroscopic precession can take any angle and the gyroscopic equations cannot necessarily be regarded as linear)

A detailed description of the principal of operation, system advantages and the prototype design is given in Section II. The experimental setup and investigations are described in Section III and the results and discussion of results are presented in Section IV.

II. SYSTEM DESCRIPTION

A. Principal of Operation

A schematic of the gyroscopic system is illustrated in Fig.1. The system, which is based on control moment gyroscope (CMG) principles, utilises the gyroscopic response of a gimballed flywheel mounted within an AUV body to generate energy from the wave induced rotational motions of the vehicle.

The system equations of motion can be described by the Newton-Euler equations. Defining $\underline{\omega}_f$ and $\underline{I}_f$ as the flywheel angular velocities and mass moment of inertias of the flywheel, with respect to (X_f, Y_f, Z_f), the angular momentum of the flywheel can be expressed as;

TABLE II
EXAMPLE POWER CONSUMPTION OF VARIOUS TORPEDO STYLE BATTERY POWERED AUVS [56]

Vehicle	Mass [kg]	Length [m]	Diameter [cm]	Stored Energy [kWh]	Endurance [Hours]	Power [W]
Iver2-580-S	20.5	1.52	14.7	0.6	14	43
Folaga AUV	31.0	2.04	16.0	0.5	6	90
REMUS 100-S	38.5	1.60	19.0	1.0	10	100
REMUS 600	240.0	3.25	32.4	5.2	70	74
Bluefin 12D	260.0	4.32	32.0	7.5	30	250
Dorado class AUV	680.0	5.30	53.0	11.0	17.5	629
Bluefin 21	750.0	4.93	53.0	13.5	25	540
Abyss AUV	880.0	4.00	66.0	11.2	24	467
REMUS 6000	884.0	3.84	71.0	11.8	22	536
Eagle Ray AUV	940.0	4.60	69.0	29.4	30	979
Explorer-class MARUM SEAL AUV	1300.0	5.50	74.0	14.0	19	737
Echo Surveyor IV	1450.0	5.40	100.0	45.0	50	900

$$\underline{H}_f = \underline{I}_f \underline{\omega}_f \tag{1}$$

In the (AUV) body fixed axis (X_b, Y_b, Z_b) this can be expressed as;

$$\underline{H}_{b*} = \underline{A}_f^b \, \underline{H}_f \tag{2}$$

where $\underline{A}_f^b$ represents the rotation matrix describing the transformation of the momentum component from (X_f, Y_f, Z_f) to (X_b, Y_b, Z_b). Including the AUV motion, the moments acting around each axis in the AUV body-fixed coordinate frame (X_b, Y_b, Z_b) can then be expressed as;

$$\underline{\dot{H}}_b = \underline{\dot{H}}_{b*} + \underline{\Omega}^{\times} \underline{H}_{b*} \tag{3}$$

where $\underline{\dot{H}}_b$, represents the moments acting around each axis in the (AUV) body-fixed coordinate frame, $\underline{\Omega}^{\times}$ represents the skew-symmetric form (equivalent to the cross product operation) of the (AUV) body motions experienced by the flywheel. $\underline{H}_{b*}$ represents angular momentum of the flywheel in the AUV body fixed axis system (X_b, Y_b, Z_b). Assuming, as illustrated in Fig.1, the flywheel is restricted about the x-axis (X_f), precesses about the z-axis (Z_f) and has an angular velocity, $\dot{\psi}$, about the y-axis (Y_f) and the flywheel and AUV centres of mass lie at the origin of the body-frames of reference and the body-frames of reference coincide with the principal axes of inertia of the bodies. As shown in [53], Equation 3 can be expanded yielding the torque about the precession axis $(Z_f = Z_b)$;

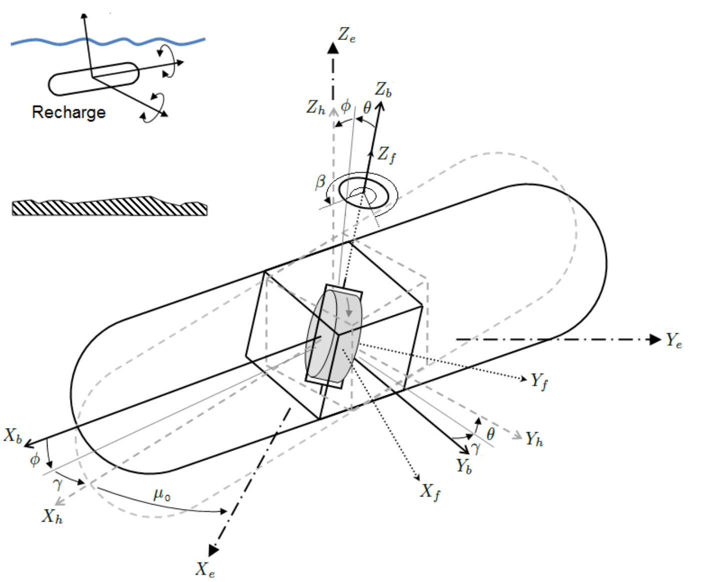

Fig. 1. System schematic and coordinate frame definitions ((X_e, Y_e, Z_e) represents an Earth fixed inertial axis system, (X_h, Y_h, Z_h) represents the hydrodynamic or equilibrium axis system that moves with the average motion of the AUV but is not fixed to the AUV, (X_b, Y_b, Z_b) represents the body (AUV) fixed axis system, (X_f, Y_f, Z_f) represents the flywheel axis system. This axis precesses but does not spin with the flywheel).

This article has been accepted for publication in a future issue of this journal, but has not been fully edited.
Content may change prior to final publication in an issue of the journal. To cite the paper please use the doi provided on the Digital Library page.

$$\tau_p = I_{zz}\ddot{\beta} - I_{yy}\dot{\psi}\dot{\phi}sin\beta + I_{yy}\dot{\psi}\dot{\theta}cos\beta \quad (4)$$

Here I_{xx}, I_{yy}, I_{zz} represents the mass moment of inertia about the flywheel fixed axis, spin axis and precession axis respectively. $\dot{\psi}$ represents the flywheel spin rate and $\dot{\theta}, \dot{\phi}$ represent the roll and pitch angular velocities of the AUV body. τ_p, β represent the torque about the precession axis and the precession angle respectively. Equation 3 shows that with AUV roll and pitch motions ($\dot{\theta}, \dot{\phi}$) a gyroscopic precession ($\dot{\beta}$) and a precession torque (τ_p) is experienced. That is, with precession motion and precession torque, the precession axis can be used to drive a generator and produce power.

B. System Advantages (and disadvantages)

The system utilises the reaction of a spinning wheel under an input torque (AUV motion) to provide an output torque of greater magnitude, orthogonal to the input torque axis and the spin axis to drive a generator. This provides a means to harvest energy in-situ with no external appendages, avoiding any additional hydrodynamic drag. Furthermore, with no direct exposure to the marine environment the system is not susceptible to environmental performance degradations i.e., bio fouling and would not be limited to daylight recharging and night time missions. Potentially the system could be applied to any rotational excited platform(s) e.g., ASVs, boats, buoys, WECs.

In practice as the effect of surface waves and swell diminishes with depth [49], similar to solar based AUVs (e.g., SAUV II), the AUV system would need to surface to recharge, as depicted in Fig.1 - admittedly exposing the AUV to the potentially hazardous wave environment. However, as waves are a concentrated form of solar energy (formed by winds passing over bodies of water created by the differential heating of air masses by the sun on the earths atmosphere) with a reported spatial concentration of time-averaged power flow of typically 0.1 - 0.3 kW/m^2 (solar) to 0.5 kW/m^2 (wind) to 2 - 3 kW/m^2 (wave) [40], greater energy capture is anticipated compared to solar and wind strategies.

C. Prototype Design

The prototype design is illustrated in Fig.2. Based on the majority of AUV systems, a torpedo style AUV, with a cylindrical body design was selected. The body diameter ($\approx 30cm$) was approximately based on the REMUS 600 AUV, see Table II. To minimise the swept volume and mass, the flywheel was designed to precess about the central axis of the flywheel, with the flywheel thickness comparable to the flywheel diameter, with an I shape cross section. The gyroscopic system was designed to allow full, unrestricted 360^o precession motion. This was achieved by using a slip ring mounted on the precession axis to provide power to the spin motor. To convert the mechanical power to electrical power a DC generator (motor) was employed. A discussion of the generator efficiency is given in Section IV-E. A summary of the AUV, gyroscopic unit and generator particulars are presented in Table III.

TABLE III
SYSTEM PARTICULARS

AUV System Particulars	**Value**
Overall length (L_b)[m]	2
Diameter [m]	0.2929
Assembled AUV Prototype Mass [kg]	110.3
Trim Angle [degrees]	11.8
Gyroscopic System Particulars	
Gyroscopic unit mass (including end plate) [kg]	11.2
Gyroscopic unit mass (excluding end plate) [kg]	6.3
Flywheel mass [kg]	3.6
Flywheel diameter [m]	0.1
Flywheel mass moment of inertia (I_{yy}) [kgm^2]	0.00482
Flywheel mass moment of inertia (I_{xx}=I_{zz}) [kgm^2]	0.00363
Generator System Particulars	
Speed constant [rpm/V]	1040
Torque constant [mNm/A]	9.18
Terminal resistance [Ω]	1.01
Speed/torque gradient [rpm/mNm]	114
Gearing (Gyroscopic precession to generator shaft)	1:73.3
Resistor (across terminals) (V_r) [Ω]	15

III. Experimental Setup and Investigations

A series of regular wave tests over a range of frequencies (0.5-1.4Hz) and wave amplitudes (0.1 and 0.05m) were conducted in a towing tank with the gyroscopic system operating (within the AUV) at several spin rates (1000, 5000, 9000rpm) and with the system disabled. The prototype was tested following a conventional sea keeping methodology, with the AUV attached to the tow post of the towing tank carriage, constraining the AUV in yaw, roll, surge and sway. For comparison a series of slack moored tests were also conducted. The experimental setups are illustrated in Fig.2. The generated data was logged at $100Hz$ (using a National Instruments compactRIO). The generated power was calculated by measuring the voltage (V_r) across a resistor (R_r) connected to the terminals of the generator i.e., $P = V_r^2/R_r$. The generator particulars are summarised in Table III.

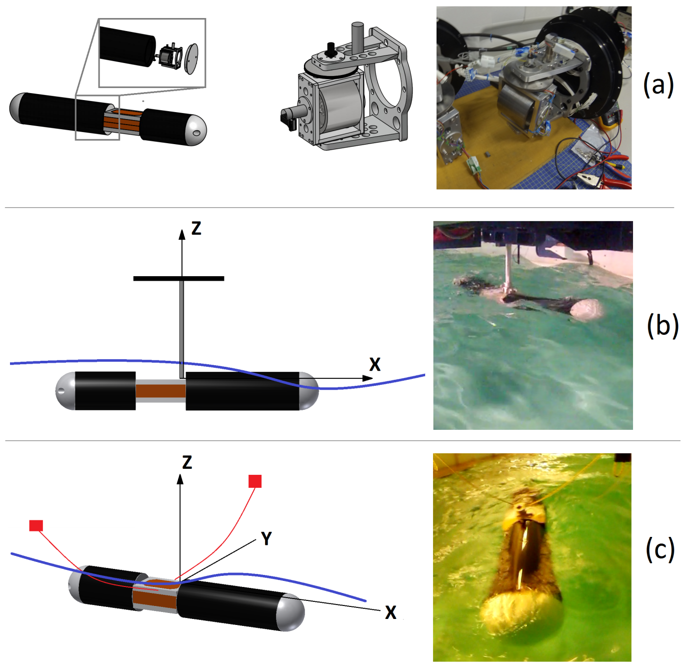

Fig. 2. Prototype system and experimental setups ((a) CAD assembly and manufactured gyroscopic unit (b) Experimental towpost arrangement (c) Experimental slack moored arrangement)

IV. Results and Discussion

The following results are presented in this section;

- Fig.3: The equivalent harvested energy (Wh) over a range of frequencies and spin rates, per hour.
- Fig.4: The generated power (peak and rms) over a range of frequencies, spin rates, wave heights and constraints.
- Fig.5: The non-dimensional pitch response ($\phi_a/k\zeta_a$) of the AUV over a range of frequencies. That is, the AUV motion response in waves without the gyroscopic system operating.
- Fig.6: Example gyroscopic precession angle variation over time.

These results are based on 10 wave encounters. Example time and frequency domain responses are presented in Figs.7 and 8 and flywheel acceleration and deceleration profiles (on start-up and shutdown) are also presented in Fig.9.

Fig.3 shows the harvested energy per hour, calculated by integrating the power profiles over 10 wave encounters and extrapolating to a one hour period. The results show that the harvested energy is greatest around resonance, tailing off as the frequency increases.

To provide a representative comparison, as the wave amplitudes were found to vary slightly between tests, the generated power (over the 10 wave encounters) were normalised with respect to the (maximum) wave amplitude, see Fig.4. The results show that the power generated is greatest around resonance ($\approx 0.7Hz$) and rapidly reduces at higher frequencies (e.g., above $1Hz$). Furthermore the results show that the maximum instantaneous power compared to the rms power is large (up to 6 times), indicating that the generated power is not sinusoidal.

This article has been accepted for publication in a future issue of this journal, but has not been fully edited.
Content may change prior to final publication in an issue of the journal. To cite the paper please use the doi provided on the Digital Library page.

As shown in Figs.7 and 8 the generated power 'pulses', as the flywheel precesses and drives the generator. Interestingly, the pulses can vary in frequency and magnitude over time and are rarely proportional to the (regular) wave frequency. That is, the generated power is typically nonlinear. Although this finding is not unexpected (see [54]), the nonlinear responses were found to be readily achievable, particularly the case of continuous precession rotation, see Fig.6(a). As a continuous precession motion can be achieved, a continuous power output is possible with the system. With a 1 degree of freedom excitation it is known that when the flywheels orientate themselves in line with the forcing excitation, no gyroscopic precession can occur and no energy can be harvested [54]. In practise it is anticipated that any slight additional axial excitation will 'kick' the system out of these dead zones and this may account for the irregular power output. Furthermore, these results indicate that an optimised restoring term and/or control of the gyroscopic precession (position and rate) could further increase the energy harvested and widen the operating range.

A. Spin Rate

With low spin rates, e.g., $1000rpm$, the gyroscopic torque is small and no significant power is generated. Generally increasing the spin rates, greater powers (peak and rms) were observed. However, the difference between $5000rpm$ and $9000rpm$ does not appear to represent a significant step change in the generated power. At these spin rates, the system response can become nonlinear and it is expected that the flywheel orientation is not always optimally aligned with the wave induced excitation, reducing the energy capture (see Fig.6(b)), and that there is an optimal spin rate for a given condition and system setup.

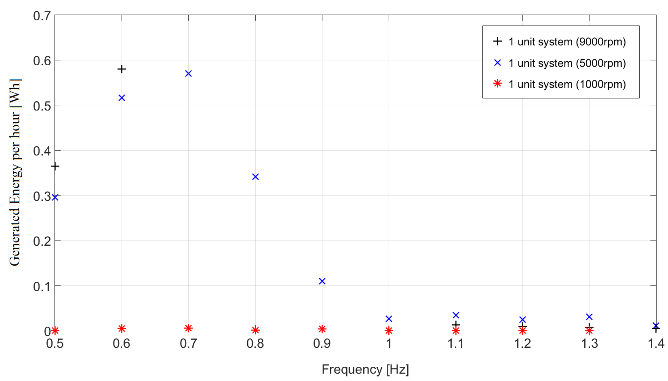

Fig. 3. The equivalent harvested energy (Wh per hour) over a range of frequencies, spin rates ($\zeta_a \approx 10cm$)

B. AUV Motion

Fig.5 shows the non-dimensional pitch response, a measure of the pitch amplitude relative to the wave slope, of the AUV prototype. This was calculated from the pitch angular velocity amplitude i.e., $\dot{\phi}_a = \phi_a \omega$, $k = \omega^2/g$. The pitch angular velocity, $\dot{\phi}$, was measured with a xSENS MTi-100 inertial measurement unit. The response shows a characteristic resonance response, around $0.7Hz$, with the motion amplitude decreasing with increasing frequency. For the investigated conditions the AUV motion responses are relatively small, with the larger investigated case ($\zeta_a \approx 10cm$) equating to a peak pitch amplitude response of approximately 7.5 degrees. That is, the test conditions represent a relatively benign sea state and AUV response. As shown by Fig.4(b), greater power can be generated in larger waves. Therefore in a real seaway, where larger waves and responses are expected, it is anticipated that greater power can be generated from the system than presented.

C. Experimental Setup

The prototype was tested following a conventional sea keeping methodology, with the AUV attached to the tow post of the towing tank carriage, constraining the AUV in yaw, roll, surge and sway. Varying the experimental constraint, Fig.4(c) the results were found to be similar in magnitude for a slack moored and tow post constrained setup. The results provide some confidence that the constraint does not significantly influence the system. However, the constraint is believed to influence the system response and a more detailed study is needed to identify the effect(s).

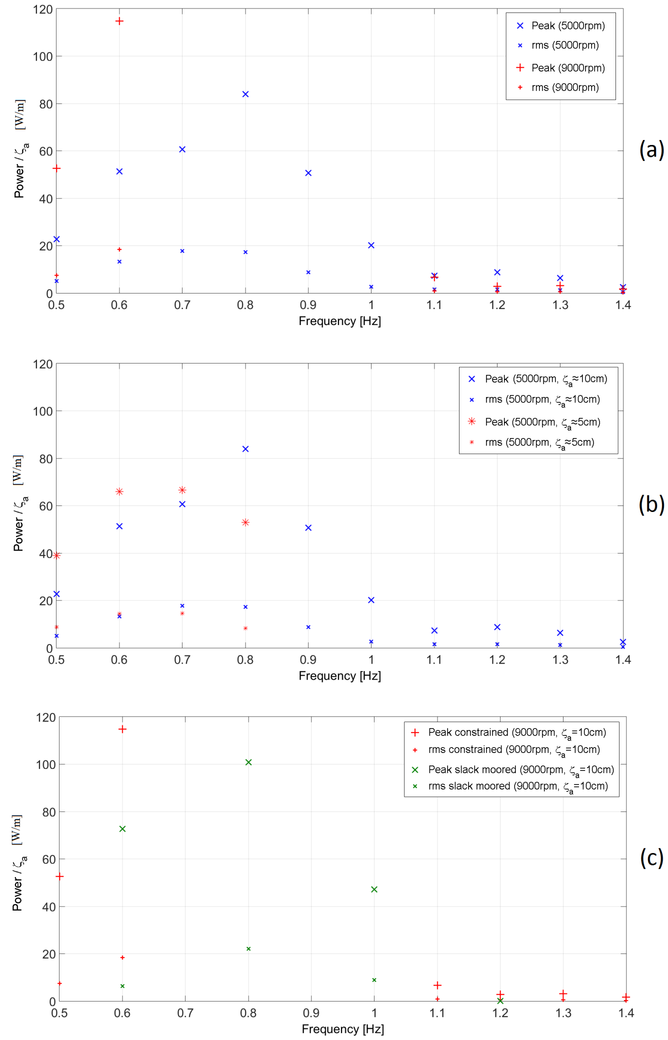

Fig. 4. Peak and rms generated power ((a) over a range of frequencies and spin rates ($\zeta_a \approx 10cm$, $5000rpm$ and $9000rpm$) (b) over a range of frequencies and wave heights ($\zeta_a \approx 5cm$ and $\approx 10cm$, $5000rpm$) (c) with tow-post and slack moored constraints ($\zeta_a \approx 10cm$, $9000rpm$)

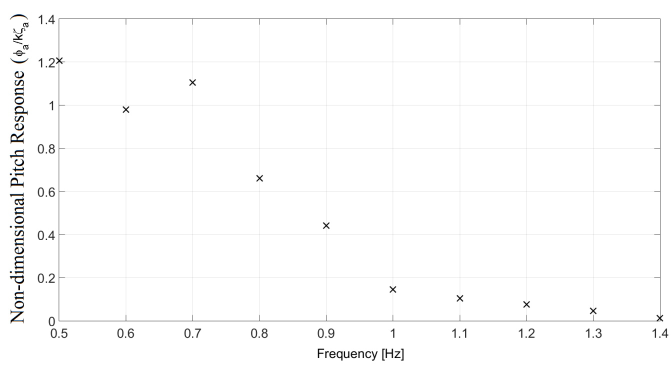

Fig. 5. Non dimensional pitch response ($\phi_a/k\zeta_a$) of the AUV in regular waves (system off)

D. Energy Balance

Fig.9 shows an example acceleration and deceleration profile for the prototype. As the system requires power to initially accelerate and then maintain the flywheel spin rate, overcoming friction, an estimate of the input power to accelerate the flywheel and the power to overcome friction and maintain the flywheel rpm was made.

Assuming a constant energy loss, the power loss due to friction (to maintain the flywheel rpm) was estimated as;

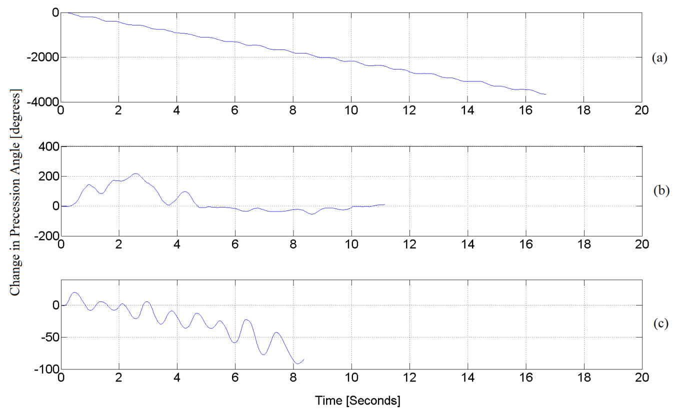

Fig. 6. Change in precession angle over time ($\zeta_a \approx 10cm$, $5000rpm$, 10 wave encounters (a) $0.6Hz$ (b) $0.9Hz$ (c) $1.2Hz$)

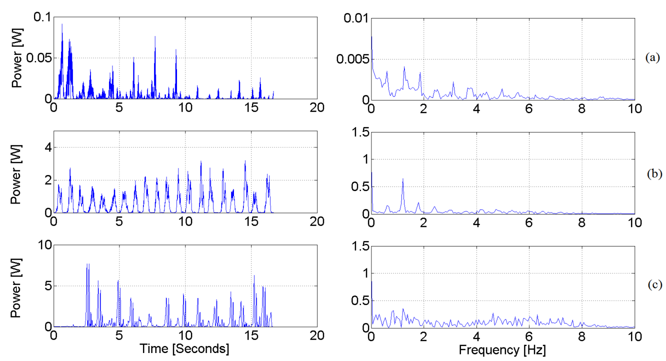

Fig. 7. Example time histories and fast Fourier transforms (fft) of generated power ($\zeta_a \approx 10cm$, $0.6Hz$ (a) $1000rpm$ (b) $5000rpm$ (c) $9000rpm$)

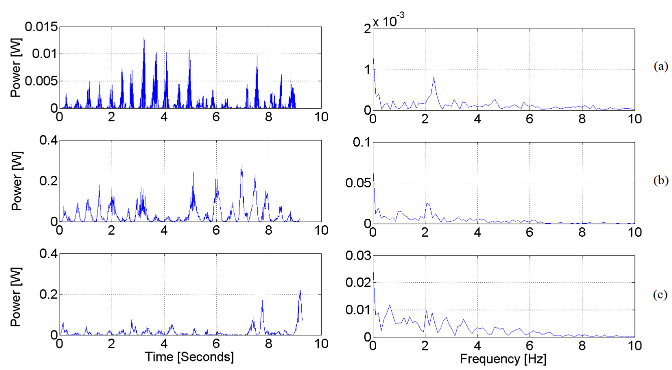

Fig. 8. Example time histories and fast Fourier transforms (fft) of generated power ($\zeta_a \approx 10cm$, $1.1Hz$ (a) $1000rpm$ (b) $5000rpm$ (c) $9000rpm$)

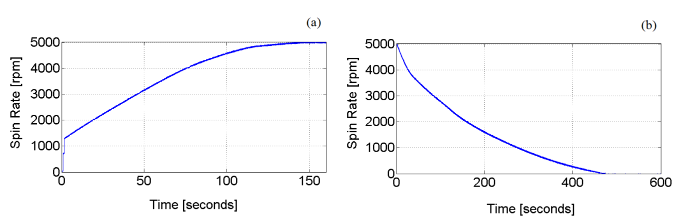

Fig. 9. Flywheel acceleration and deceleration profiles ((a) Flywheel spun up to $5000rpm$ (b) Flywheel spun down from $5000rpm$)

$$P = \frac{1}{2} I_{yy} \omega_f^2 / t \tag{5}$$

TABLE IV
COMPARISON TO OTHER ENERGY SCAVENGING SYSTEMS

Prototype Gyroscopic System	Power	Notes
Power (actual)	up to 0.8-1.2 W (rms) 3.2-8 W (peak)	$\dot{\psi} = 5000 - 9000rpm$ (note: $\zeta_a < 10cm$) (ignoring frictional losses)
Power per wave amplitude	up to $20W/m$ (rms) 80-115W/m (peak)	$\dot{\psi} = 5000 - 9000rpm$, $\zeta_a \approx 10cm$ (ignoring frictional losses)
Power (maximum - if $\eta_{pto} = 100\%$)	up to 2.6-4.1 W (rms) 10.7-26.7 W (peak)	$\dot{\psi} = 5000 - 9000rpm$ (note: $\zeta_a < 10cm$) (ignoring frictional losses)
Other Systems	**Power**	**Notes**
SOLO-TREC (thermal) [57]	1.6W	6100 joules per dive, assumed one hour dive
SAUVII (solar) [25]	7.5-22.5W	300Wh - 900Wh per day, scaled to AUV footprint ($0.6m^2$)
Waveglider (solar) [17]	≈8.6W	Solar panel peak power, assumed 20% efficiency and scaled to AUV footprint ($0.6m^2$)
Forgen 500NT (Small wind turbine) [32]	10W	Nominal output, 15 knots, 7kg, 200mm diameter
Autonaut (solar) [5]	≈10W	Solar panel peak power, assumed 20% efficiency and scaled to AUV footprint ($0.6m^2$)
C-enduro (solar) [4]	≈14.2W	Solar panel peak power, assumed 20% efficiency and scaled to AUV footprint ($0.6m^2$)
Leading Edge LE-v50 (Small wind turbine) [32]	14W	Nominal output, 15 knots, 9kg, 290mm diameter
Forgen 1000NT (Small wind turbine) [32]	15W	Nominal output, 15 knots, 15kg, 300mm diameter

where $\frac{1}{2}I_{yy}\omega_f^2$ represents the stored kinetic energy in the flywheel. As the prototype system takes approximately 470 seconds for the flywheel to slow from $5000rpm$ to rest, see Fig.9(b), the power loss due to friction was estimated as;

$$P = (0.5 \times 0.00482 \times (5000 \times 2\pi/60)^2)/470 \approx 1.4W$$

That is, a continuous power input of $1.4W$ (estimate) was required to maintain the flywheel at its operating spin rate. Similarly, the input power to accelerate the flywheel was calculated, see Fig.9(a), yielding approximately a $4W$ power demand for a 160 second start up time, assuming no losses. Considering the supplied current was limited to 4A and 24V ($\approx 100W$), or considering the motor rating ($40W$), the efficiency of start-up of the prototype system is estimated at between $4 - 10\%$.

E. Generator Efficiency

Expressing the generator overall efficiency as the ratio of electrical power output, P_e, to the mechanical power input, P_m:

$$\eta_{pto} = \frac{P_e}{P_m} \tag{6}$$

and estimating the electrical and mechanical power delivered to the generator as;

$$P_e = \frac{V^2}{R} \tag{7}$$

and

$$P_m = \frac{\tau_p}{g} g\dot{\beta} \tag{8}$$

respectively, where $\frac{\tau_p}{g}$ and $g\dot{\beta}$ represents the torque and angular velocity at the generator shaft and g represents the gearing between the gyroscopic precession axis and the generator shaft. Inaddition, estimating the magnitude of the gyroscopic torque τ_p, as;

$$\tau_p \approx I_{yy}\dot{\psi}\dot{\phi} \tag{9}$$

Then, the estimated mechanical power delivered to the generator shaft (using the rms and maximum measured values for V, $\dot{\phi}$ and $\dot{\beta}$), as shown in Figure 10 (for a spin rate of $5000rpm$), is between $0.05 - 4W$ rms and $0.4 - 18W$ peak. In comparison the electrical power ranged from $0.02 - 0.8W$ rms and $0.14 - 3.2W$ peak. That is, the estimated efficiency of the prototype generator is estimated to be $\approx 30\%$ (ranging between $14 - 50\%$), as shown in Figure 10.

In the tested conditions the prototype system generated power up to 0.8 rms (3.2 peak)W with $\dot{\psi} = 5000rpm$ and up to 1.24 rms (8 peak)W with $\dot{\psi} = 9000rpm$ (see Figure 10). This shows that the system can harvest energy, however, given the estimated power loss due to friction in the tested conditions a net gain may not have been achieved. Given that the investigated conditions and responses were relatively small and that the estimated mechanical energy delivered to the generator shaft is typically greater than the friction loss (see Figure 10). Then a net gain appears readily feasible with operation in larger waves and/or improved generator efficiency (for example if $\eta_{pto} = 100\%$ (instead of $\approx 30\%$) then the system could be expected to generate up to 2.67 rms(10.67 peak) W with $\dot{\psi} = 5000rpm$ and up to 4.12rms (26.67 peak) W with $\dot{\psi} = 9000rpm$). This could be achieved by controlling the torque and rpm delivered to the generator, for example through the use of a controlled, variable gearing between the precession axis and generator shaft. Compared to other energy scavenging systems, Table IV, and AUV powering requirements, Table I and II, the results are very encouraging.

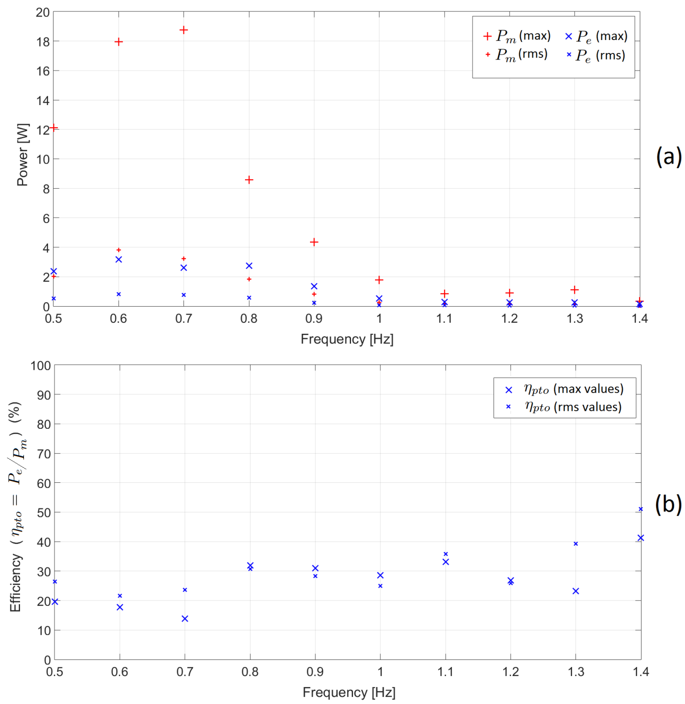

Fig. 10. Generator efficiency ((a) Mechanical (P_m) and electrical power (P_e) (b) Percentage efficiency)

V. Conclusions

This paper describes a novel prototype energy scavenging system for a torpedo style AUV. The system, based on control moment gyroscope principles, provides a means to harvest (wave) energy in-situ, internally, without external appendages. A description of the system operation, design and experimental results from a series of regular wave tests conducted at zero speed in a towing tank are presented. The results show that the system can harvest energy, although in the tested conditions a net energy gain was not achieved. In the tested conditions ($\zeta_a \approx 10cm$), equating to a maximum (AUV) pitch response of 7.5 degrees, the prototype system harvested the equivalent of between 0.05-0.6Wh per hour, with a maximum recorded peak power of 8W. The generated power was found to be greatest around resonance, tailing off as the wave frequency increased. Typically, greater spin rates and wave amplitudes yielded greater power with the response becoming increasingly nonlinear.

The experimental results show that the system has the potential to provide additional hotel load or power specific systems on an AUV or similarly rotationally excited platform, e.g., Autonomous Surface Vessels (ASVs), buoys or boats.

Acknowledgment

This research was funded by the Defence Science and Technology Laboratory (DSTL) through the Centre for Defence Enterprise (CDE).

References

[1] 2200-s, survey quality sonars for small auvs, product information. [Online]. Available: http://auvac.org/uploads/manufacturer_spec_sheet_pdf_sonar/EdgeTech%202200-s_brochure.pdf
[2] 2d imaging sonar data sheet. [Online]. Available: http://auvac.org/uploads/manufacturer_spec_sheet_pdf_sonar/Data_Sheet_P900-90_v2.pdf
[3] Aquadopp current meter product brochure. [Online]. Available: http://www.nortek-as.com/lib/brochures/aquadopp-current-meter
[4] Asv c-enduro. long endurance marine unmanned surface vehicle (lemusv) product brochure. [Online]. Available: http://www.asvglobal.com/files/datasheets/c-enduro-datasheet.pdf
[5] Autonaut specifications. [Online]. Available: http://www.autonautusv.com/specifications

[6] Avtrak 2 (omni-directional version) data sheet. [Online]. Available: http://auvac.org/uploads/manufacturer_spec_sheet_pdf_sonar/sonardyne_8065_avtrak2.pdf
[7] Avtrak 6 (omni-directional version) data sheet. [Online]. Available: http://auvac.org/uploads/manufacturer_spec_sheet_pdf_nav/Sonardyne_8220_av6.pdf
[8] Cyclops-6k submersible sensors specification sheet. [Online]. Available: http://www.turnerdesigns.com/products/submersible-fluorometer/cyclops-6k-6000-meter-submersible-fluorescence-and-turbidity-sensors
[9] Dc-4e digital compass. [Online]. Available: http://www.spartonnavex.com/product/dc-4e/
[10] Explorer pa doppler velocity log (dvl) brochure. [Online]. Available: http://auvac.org/uploads/manufacturer_spec_sheet_pdf_nav/explorer_ds_lr.pdf
[11] High resolution ccd camera data sheet. [Online]. Available: http://www.alliedvisiontec.com/us/products/cameras/gigabit-ethernet/prosilica-ge/ge1900.html
[12] Imagenex model 853 scientific echo sounder with data logger specification sheet. [Online]. Available: http://auvac.org/uploads/manufacturer_spec_sheet_pdf_sonar/Imagenex%20853_ES_with_Data_Logger_Specs_rev4.pdf
[13] Kongsberg geoacoustics wide swath bathymetry for auvs, product information. [Online]. Available: http://auvac.org/uploads/manufacturer_spec_sheet_pdf_sonar/GeoSwath-ROV-AUV.pdf
[14] L-3 nautronix, high precision timing reference (hptr) performance specification sheet. [Online]. Available: http://auvac.org/uploads/manufacturer_spec_sheet_pdf_nav/HPTR_Rev_2.1.pdf
[15] L-3 oceania gpm300 acoustic modem, data sheet. [Online]. Available: http://www2.l-3com.com/oceania//pdfs/datasheets/GPM%20300%20Acoustic%20Modem%20Spec%20Sheet%20Rev%201%206.pdf
[16] Lbl positioning and communication systems: product information guide. [Online]. Available: http://auvac.org/uploads/manufacturer_spec_sheet_pdf_nav/EvoLogics_S2CR_LBL_a4.pdf
[17] Liquid robotics product specifications. wave glider sv2. [Online]. Available: http://www.ofeg.org/np4/file/66/2013_Liquid_Robotics_Wave_Gliders_SV2.pdf
[18] Mb1350-45, 3d ultra-high resolution microbathymetry brochure. [Online]. Available: http://auvac.org/uploads/manufacturer_spec_sheet_pdf_sonar/MB1350-45_v2.pdf
[19] Microrider-1000 modular, self-contained turbulence profiler data sheet. [Online]. Available: http://www.rocklandscientific.com/LinkClick.aspx?fileticket=2QpE2AQoUco%3d&tabid=133
[20] The microtransat challenge. [Online]. Available: http://www.microtransat.org/
[21] Ocean aero. unmanned underwater/surface vessel uusv product brochure. [Online]. Available: http://www.oceanaero.us/OAHandout9.pdf
[22] Paroscientific series 9000 pressure instrument. [Online]. Available: http://auvac.org/sensors/view/23?from_search=1
[23] Sbe 49 fastcat ctd sensor specification sheet. [Online]. Available: http://www.seabird.com/sbe49-fastcat-ctd
[24] Sea scan pc auv specification sheet. [Online]. Available: http://www.marinesonic.us/products/SSPCAUV/sspc-auv-documents/Sea%20Scan%20PC%20AUV%20Specifications.pdf
[25] Solar-powered auv: Sauvii white paper. [Online]. Available: http://www.falmouth.com/images/SAUVwhitePaper.pdf
[26] Sparton phod-1 hydrophone specification. [Online]. Available: http://www.spartonnavex.com/product/phod-1-hydrophone/
[27] Suna v2 uv nitrate sensor specification sheet. [Online]. Available: http://satlantic.com/suna?qt-product_tabs=1#qt-product_tabs
[28] Uls-500 underwater laser scanner for long range scans, product brochure. [Online]. Available: https://www.oceanologyinternational.com/__novadocuments/18127?v=634886964440300000
[29] Valeport ultra sv (sound velocity sensor) specification sheet. [Online]. Available: http://www.valeport.co.uk/Portals/0/Docs/Datasheets/Valeport_ultraSV_v2a.pdf
[30] Wfs technologies: Seatooth s200 underwater rf, product information. [Online]. Available: http://auvac.org/comms/view/6?from_search=1
[31] xsens mti 100-series brochure. [Online]. Available: https://www.xsens.com/wp-content/uploads/2013/12/MTi-100-series1.pdf
[32] (2013, March) Practical boat owner. we got the power! wind turbines: a buyers guide. [Online]. Available: http://www.ampair.com/sites/all/files/product/resources/PBO%20Magazine.pdf
[33] G. Bracco, E. Giorcelli, F. Marignetti, and G. Mattiazzo, "ISWEC: Application of linear tubular generators," *IEEE International Symposium on Industrial Electronics*, pp. 2426–2430, 2010.
[34] G. Bracco, E. Giorcelli, and G. Mattiazzo, "ISWEC: A gyroscopic mechanism for wave power exploitation," *Mechanism and Machine Theory*, vol. 46, no. 10, pp. 1411 – 1424, 2011.
[35] G. Bracco, E. Giorcelli, G. Mattiazzo, M. Pastorelli, and J. Taylor, "ISWEC: design of a prototype model with gyroscope," *International Conference on Clean Electrical Power*, pp. 57–63, 2009.
[36] R. Button, J. Kamp, T. Curtin, and J. Dryden, "A survey of missions for unmanned undersea vehicles," *NATIONAL DEFENSE RESEARCH INSTITUTE, The RAND Corporation*, 2009.
[37] R. Camilli, A. Bowen, and N. Farr, "Bright Blue: Advanced technologies for marine environmental monitoring and offshore energy," *OCEANS '10*, 2010.
[38] D. Crimmins, C. Patty, M. Beliard, J. Baker, J. Jalbert, R. Komerska, S. Chappell, and D. Blidberg, "Long-endurance test results of the solar-powered AUV system," *OCEANS '06*, pp. 1–5, 2006.
[39] R. Davis, C. Eriksen, and P. Jones, "Autonomous buoyancy-driven underwater gliders," *The Technology and Applications of Autonomous Underwater Vehicles*, pp. 37–58, 2002.
[40] J. Falnes, "A review of wave-energy extraction," *Marine Structures*, vol. 20, no. 4, pp. 185 – 201, 2007.
[41] G. Griffiths, J. Jamieson, S. Mitchell, and K. Rutherford, "Energy storage for long endurance AUVs," *Proceedings of Advances in Technology for Underwater Vehicles, London, UK*, pp. 8–16, 2004.
[42] G. Griffiths, D. Reece, P. Blackmore, M. Lain, S. Mitchell, and J. Jamieson, "Modeling hybrid energy systems for use in AUVs," *Proc. 14th Unmanned Untethered Submersible Technology (UUST)*, 2005.
[43] G. Hagerman, "Wave energy systems for recharging AUV energy supplies," *Proceedings of the Symposium on Autonomous Underwater Vehicle Technology*, pp. 75–84, 2002.
[44] W. A. Hermann, "Quantifying global exergy resources," *Energy*, vol. 31, no. 12, pp. 1685 – 1702, 2006. [Online]. Available: http://www.sciencedirect.com/science/article/pii/S0360544205001805
[45] T. Hyakudome, T. Aoki, T. Murashima, S. Tsukioka, H. Yoshida, H. Nakajoh, T. Ida, S. Ishibashi, and R. Sasamoto, "Key technologies for AUV 'URASHIMA'," *OCEANS '02 MTS/IEEE*, vol. 1, pp. 162–166, 2002.
[46] H. Kanki, "Gyro wave activated power generator and a wave suppressor using the power generation, patent US 7,003,947 B2," 2006.
[47] H. Kanki, S. Arii, T. Furusawa, and T. Otoyo, "Development of advanced wave power generation system by applying gyroscopic moment," *Proceedings of the 8th European Wave and Tidal Energy Conference (EWTEC), Uppsala, Sweden*, pp. 280–283, 2009.
[48] H. Kanki, T. Morimoto, M. Kawanishi, T. Onishi, and T. Hata, "Study on dynamics of floating wave-power generating system using gyro moment," *The Japan Society of Mechanical Engineers*, vol. 80, pp. 6.57–6.58, 2005.
[49] E. Levine, L. Goodman, and C. Lubke, "AUV-based swell characterization," *IEEE/OES Autonomous Underwater Vehicles*, pp. 1–6, 2008.
[50] A. Mendez, T. Leo, and M. Herreros, "Current state of technology of fuel cell power systems for autonomous underwater vehicles." *Energies*, vol. 7(7), pp. 4676–4693, 2014.
[51] G. Reader, J. Potter, and J. Hawley, "The evolution of AUV power systems," *OCEANS '02 MTS/IEEE*, vol. 1, pp. 191–198, 2002.
[52] F. Salcedo, P. Ruiz-Minguela, R. Rodriguez, P. Ricci1, and M. Santos, "OCEANTEC: Sea trials of a quarter scale prototype," *Proceedings of 8th European Wave Tidal Energy Conference (EWTEC), Uppsala, Sweden*, p. 460465, 2009.

[53] N. Townsend and R. Shenoi, "A gyroscopic wave energy recovery system for marine vessels," *IEEE Journal of Oceanic Engineering*, vol. 37(2), pp. 271–280, 2012.
[54] ——, "Modelling and analysis of a single gimbal gyroscopic energy harvester," *Nonlinear Dynamics*, vol. 72(1), pp. 285–300, 2013.
[55] C. wei Zheng and J. Pan, "Assessment of the global ocean wind energy resource," *Renewable and Sustainable Energy Reviews*, vol. 33, no. 0, pp. 382 – 391, 2014. [Online]. Available: http://www.sciencedirect.com/science/article/pii/S1364032114000860
[56] R. Wynn, E. Linley, and J. Hunt. Global inventory of auv and glider technology available for routine marine surveying. [Online]. Available: http://www.nerc.ac.uk/innovation/activities/infrastructure/offshore/catalogue-of-auvs.pdf
[57] C. Yi, "Thermal recharging battery for underwater instrumentations," *Ocean Bottom Seismograph (OBS) Workshop, Redondo Beach, California*, 2013.
[58] C. Zheng, L. Shao, W. Shi, Q. Su, G. Lin, X. Li, and X. Chen, "An assessment of global ocean wave energy resources over the last 45 a," *Acta Oceanologica Sinica*, vol. 33, no. 1, pp. 92–101, 2014. [Online]. Available: http://dx.doi.org/10.1007/s13131-014-0418-5